CellPress

Molecular Cell
Article

XPF-ERCC1 Acts in Unhooking DNA Interstrand Crosslinks in Cooperation with FANCD2 and FANCP/SLX4

Daisy Klein Douwel,[1,4] Rick A.C.M. Boonen,[1,4] David T. Long,[2] Anna A. Szypowska,[1] Markus Räschle,[3] Johannes C. Walter,[2] and Puck Knipscheer[1,*]

[1]Hubrecht Institute-KNAW, University Medical Center Utrecht and Cancer Genomics Netherlands, Uppsalalaan 8, 3584 CT Utrecht, the Netherlands

[2]Department of Biological Chemistry and Molecular Pharmacology, Harvard Medical School, 240 Longwood Avenue, Boston, MA 02115, USA

[3]Department of Proteomics and Signal Transduction, Max Planck Institute of Biochemistry, 82152 Martinsried, Germany

[4]Co-first author

*Correspondence: p.knipscheer@hubrecht.eu

http://dx.doi.org/10.1016/j.molcel.2014.03.015

SUMMARY

DNA interstrand crosslinks (ICLs), highly toxic lesions that covalently link the Watson and Crick strands of the double helix, are repaired by a complex, replication-coupled pathway in higher eukaryotes. The earliest DNA processing event in ICL repair is the incision of parental DNA on either side of the ICL ("unhooking"), which allows lesion bypass. Incisions depend critically on the Fanconi anemia pathway, whose activation involves ubiquitylation of the FANCD2 protein. Using *Xenopus* egg extracts, which support replication-coupled ICL repair, we show that the 3′ flap endonuclease XPF-ERCC1 cooperates with SLX4/FANCP to carry out the unhooking incisions. Efficient recruitment of XPF-ERCC1 and SLX4 to the ICL depends on FANCD2 and its ubiquitylation. These data help define the molecular mechanism by which the Fanconi anemia pathway promotes a key event in replication-coupled ICL repair.

INTRODUCTION

DNA interstrand crosslinks (ICLs) are extremely toxic DNA lesions because they covalently connect the two strands of the DNA double helix, thereby blocking DNA replication and transcription. The primary mechanism of ICL repair is coupled to DNA replication in S phase, while a secondary mechanism acts outside of S phase (Räschle et al., 2008; Williams et al., 2012). Replication-dependent ICL repair involves the collaboration of factors involved in nucleotide excision repair (NER), translesion DNA synthesis (TLS), and homologous recombination (HR). Additionally, the Fanconi anemia (FA) pathway protects higher eukaryotic cells from ICLs (Kim et al., 2012). Mutations in any one of 15 FA genes causes FA, which is characterized by developmental abnormalities, bone marrow failure, cancer susceptibility, and cellular sensitivity to ICL-inducing agents. Accumulating evidence indicates that the FA proteins are directly involved in the repair of ICLs (Howlett et al., 2002; Knipscheer et al., 2009; Thompson and Hinz, 2009), but much remains to be learned about their molecular role and interaction with other repair factors. A key event in the activation of the FA pathway is the ubiquitylation of FANCI-FANCD2 by the Fanconi core complex, a multisubunit E3 ubiquitin ligase consisting of FANCA, B, C, E, F, G, L, M, and the accessory proteins FAAP20, FAAP24, and FAAP100. The remaining five FA proteins, FANCD1, J, N, O, and P are thought to function downstream or independently of FANCI-FANCD2 ubiquitylation (Kottemann and Smogorzewska, 2013).

Using *Xenopus* egg extracts, we recently developed a system that recapitulates replication-coupled and FANCI-FANCD2-dependent ICL repair in vitro (Knipscheer et al., 2012; Räschle et al., 2008). This system allows the molecular dissection of this repair pathway under physiological conditions. In contrast to cell-based assays that involve indirect repair readouts such as cell survival or foci formation, the *Xenopus* egg extract system enables the direct examination of ICL repair. Additionally, the effects of non-ICL damage are avoided, as it makes use of a plasmid template containing a site-specific ICL. Using this approach, we showed previously (Räschle et al., 2008) that two replication forks converge on the crosslink and stall 20–40 nucleotides (nt) from the ICL (Figure 1A, step i), after which one fork advances to within 1 nt of the lesion (Figure 1A, step ii). Next, dual incisions on either side of the ICL unhook the crosslink from one DNA strand (Figure 1A, step iii), allowing a stepwise lesion bypass reaction (Figure 1A, steps iv and v). Finally, fully repaired products are generated by HR-mediated repair of the incised strand (Figure 1A, step vi) (Long et al., 2011). We also showed that the incisions that unhook the ICL are critically dependent on FANCD2 and its ubiquitylation (Knipscheer et al., 2009). However, the mechanism by which ubiquitylated FANCI-FANCD2 promotes these incisions remains unknown.

A number of nucleases have been suggested to function in ICL repair, including MUS81-EME1, XPF-ERCC1, FAN1, SLX4-SLX1, SNM1A, XPG, and FEN1. Their precise roles have not been determined, but their activity is likely important at various stages of ICL repair, including unhooking, HR, and processing

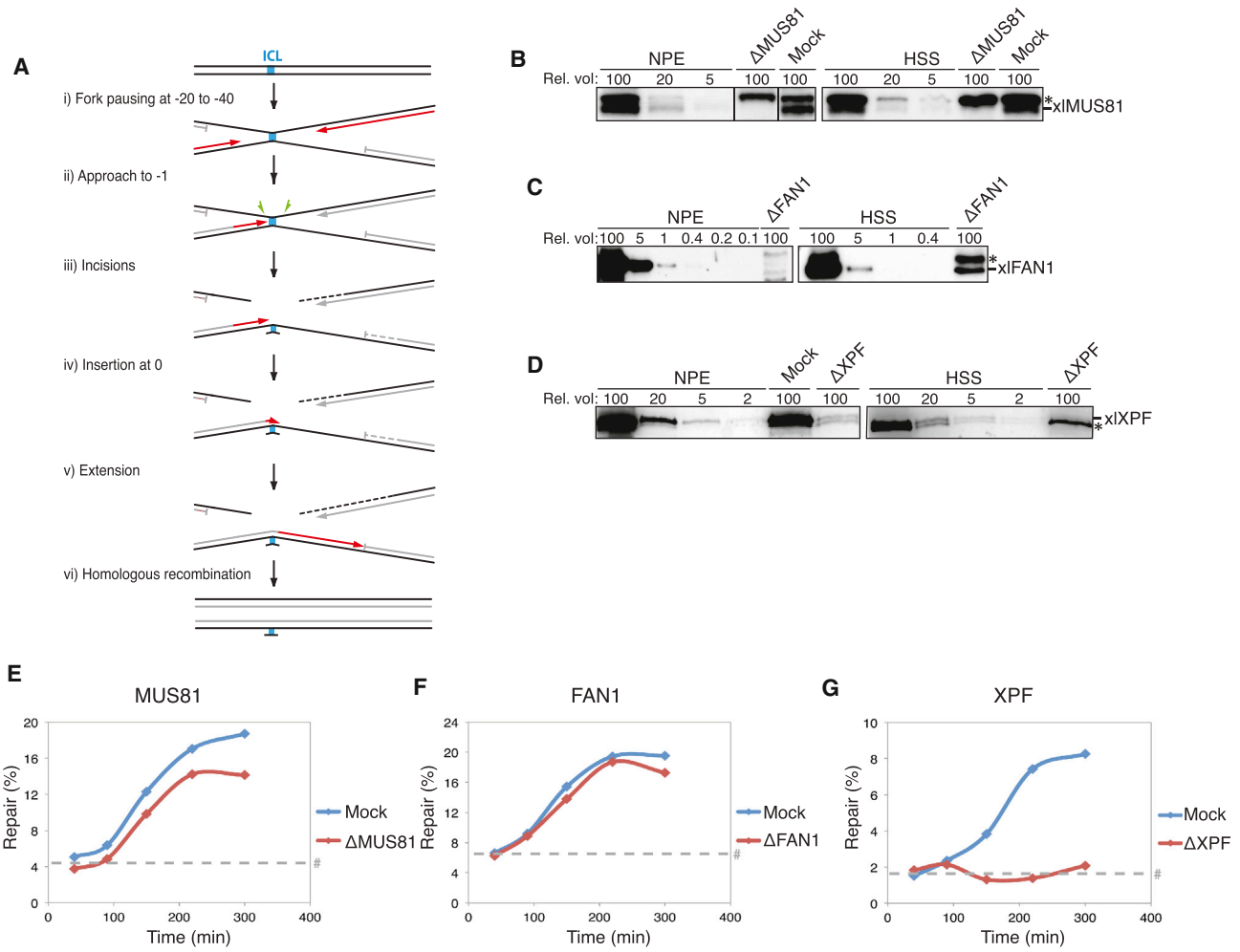

Figure 1. XPF Depletion, but Not MUS81 or FAN1 Depletion, Abrogates ICL Repair

(A) Schematic representation of ICL repair in *Xenopus* egg extract (Räschle et al., 2008).

(B) Mock- and MUS81-depleted nucleoplasmic egg extract (NPE) and high-speed supernatant (HSS) were analyzed by western blot using α-MUS81 antibody. A dilution series of undepleted extract was loaded on the same blot to determine the degree of depletion. A relative volume of 100 corresponds to 0.2 μl NPE or HSS. Line within blot indicates position where irrelevant lanes were removed.

(C) As in (B) but using α-FAN1 antibody. To reduce the level of FAN1 further, HSS was diluted in the replication reaction (see Supplemental Experimental Procedures).

(D) As in (B) but using α-XPF antibody.

(E) pICL was replicated in *Xenopus* egg extract that was mock depleted or MUS81 depleted. Replication intermediates were isolated and digested with HincII, or HincII and SapI, and separated on agarose gel. Repair efficiency was calculated and plotted.

(F) As in (E) but for mock- versus FAN1-depleted extract.

(G) As in (E) but for mock- versus XPF-depleted extract. Of note: Due to differences in depletion conditions, total repair efficiency may vary between experiments. *, background band. #, SapI fragments from contaminating uncrosslinked plasmid present in varying degrees in different pICL preparations. See also Figure S1.

and removal of the unhooked adduct (Figure 1A). Since the unhooking incisions are FA pathway-dependent and irreversibly commit the cell to ICL repair, understanding how they occur is particularly important. The asymmetric nature of the DNA structure that is the template for incisions (Figure 1A, step iii) suggests that both a 3′ and a 5′ flap endonuclease are involved in unhooking. The 3′ flap endonuclease MUS81-EME1 has been implicated in the first incision, as its depletion is reported to inhibit double-stranded break (DSB) accumulation after treatment with ICL inducing agents (Hanada et al., 2006). However, MUS81 also has functions in processing HR intermediates (Chen et al., 2001; Ciccia et al., 2008) and stalled replication forks (Osman and Whitby, 2007). XPF-ERCC1 is a 3′ flap endonuclease that is critical for NER. Importantly, XPF-ERCC1 deficiency causes high sensitivity to ICL-inducing agents, suggesting an additional role in ICL repair (De Silva et al., 2000). The absence of XPF-ERCC1 leads to persistent ICL-induced DSBs, indicating that at least one incision is made but subsequent steps are defective (De Silva et al., 2000; Niedernhofer et al., 2004). Accordingly, XPF-ERCC1 could act in the second

unhooking incision, or further downstream in HR. There are several reports supporting either of these functions (Adair et al., 2000; Bergstralh and Sekelsky, 2008; Schiestl and Prakash, 1990), but direct evidence for the role of XPF-ERCC1 in ICL repair is lacking.

The 5′ flap endonuclease FAN1 also confers resistance to ICLs and, in addition, interacts with ubiquitylated FANCD2, identifying FAN1 as an attractive candidate to perform one of the unhooking incisions (Kratz et al., 2010; Liu et al., 2010; MacKay et al., 2010; Smogorzewska et al., 2010). Yet it was recently shown that deletion of FAN1 does not lead to FA and is not epistatic with deletion of FA proteins in DT40 cells, arguing against a major role for this endonuclease in the FA pathway (Trujillo et al., 2012). Two additional 5′ endonucleases, XPG and FEN1, were shown to confer resistance to ICLs, but little is known about their involvement in ICL repair (Wood, 2010; Zheng et al., 2007). Furthermore, the exonuclease SNM1A has been suggested to act in ICL repair (Dronkert et al., 2000). In vitro assays have shown that SNM1A could be involved either in unhooking or in trimming the ends of the unhooked adduct to allow TLS (Wang et al., 2011). Finally, the SLX4-SLX1 endonuclease complex has recently been reported to play a role in ICL repair (Fekairi et al., 2009; Muñoz et al., 2009; Svendsen et al., 2009). Although deficiency of the active subunit SLX1 only leads to a mild sensitivity to ICL-inducing agents, SLX4-deficient cells are hypersensitive. In addition to interaction with SLX1, SLX4 binds MUS81-EME1 and XPF-ERCC1. Interaction of SLX4 with MUS81 seems to be dispensable for ICL repair, as loss of this interaction confers only minor sensitivity to ICLs, while loss of SLX1 interaction causes moderate sensitivity and loss of XPF interaction leads to hypersensitivity to ICL-inducing agents (Castor et al., 2013; Kim et al., 2013). The function of SLX4 and its interaction with XPF-ERCC1 during ICL repair is unclear, but the recent identification of SLX4/FANCP as a Fanconi gene underscores its importance in this process (Kim et al., 2011; Stoepker et al., 2011).

To determine which endonucleases are responsible for the incisions that unhook the ICL, we made use of *Xenopus* egg extracts. Immunodepletion of MUS81 or FAN1 from extract did not affect ICL repair. In contrast, removal of XPF-ERCC1 dramatically impaired repair efficiency due to a defect in crosslink unhooking. The ICL repair and unhooking defects were only rescued after adding recombinant XPF-ERCC1 in combination with SLX4, showing that SLX4 also functions specifically in unhooking. We further demonstrated that efficient recruitment of XPF-ERCC1 and SLX4 to ICLs depends on FANCD2. Our data unambiguously demonstrate that XPF-ERCC1 acts in the unhooking incisions of replication-coupled ICL repair, and that recruitment of this enzyme to ICLs by SLX4 is stimulated by ubiquitylated FANCD2.

RESULTS

Depletion of XPF-ERCC1, but Not MUS81 or FAN1, Inhibits ICL Repair

To investigate the role of structure-specific endonucleases in ICL repair, we employed a plasmid-based ICL repair assay using *Xenopus* egg extract (Knipscheer et al., 2012; Räschle et al., 2008). Plasmids are first incubated in a high-speed supernatant (HSS) of *Xenopus* egg cytoplasm, which supports the assembly of prereplication complexes (pre-RCs). Addition of a highly concentrated nucleoplasmic egg extract (NPE) triggers replication initiation from these pre-RCs, followed by a single, complete round of DNA replication. Replication-dependent repair of plasmid templates containing a sequence-specific cisplatin interstrand crosslink (pICL) is measured by the regeneration of a SapI restriction site that is blocked by the crosslink (Räschle et al., 2008). We raised antibodies against *Xenopus laevis* MUS81, XPF, and FAN1 (Figure S1A). All antibodies efficiently recognized the respective recombinant proteins and enabled immunodepletion of the proteins from extract (Figures 1B–1D and S1). Immunodepletion of MUS81 caused only a minor decrease in ICL repair efficiency compared to a mock-depleted extract (Figures 1E and S1C). FAN1 depletion showed no effect on ICL repair efficiency (Figures 1F and S1D). Thus, neither MUS81 nor FAN1 appears to have a major role in ICL repair in our system, although we cannot exclude that they were insufficiently depleted or that they function redundantly with other nucleases. Nevertheless, double depletion of FAN1 and MUS81 did not result in an additional repair defect, indicating that these proteins do not function redundantly (Figures S1E and S1F). Strikingly, when we immunodepleted XPF, ICL repair was completely abrogated (Figures 1G and S1G), suggesting that XPF plays a direct and crucial role in this process. XPF functions together with a regulatory subunit, ERCC1, and immunodepletion with an antibody against *Xenopus laevis* ERCC1 co-depleted XPF and vice versa (Figures S1A and S1H). These data indicate that XPF and ERCC1 form a tight complex in *Xenopus* egg extracts. Importantly, immunodepletion of ERCC1 also abrogated ICL repair (Figure S1I). Taken together, our results suggest that XPF-ERCC1 is required for replication-coupled ICL repair in *Xenopus* egg extracts.

XPF-ERCC1 Requires SLX4 for Its Function in ICL Repair

To show that the ICL repair defect after depletion of XPF/ERCC1 was specifically caused by depletion of XPF-ERCC1, we added back recombinant XPF-ERCC1. We were not able to purify *xl*XPF-*xl*ERCC1 from insect cells due to expression and solubility problems. We therefore coexpressed *Xenopus laevis* XPF and human ERCC1 in insect cells and found that these proteins form a stable complex that was readily purified (Figure 2A). The *xl*XPF-*hs*ERCC1 complex exhibited endonuclease activity similar to the *hs*XPF-*hs*ERCC1 complex using a stem-loop incision assay (Enzlin and Schärer, 2002) (Figures S2A and S2B). In contrast, the *xl*XPF^{D668A}-*hs*ERCC1 complex, containing a mutation in the active site of XPF, was unable to incise DNA (Figure S2C).

When we added recombinant *xl*XPF-*hs*ERCC1, which we refer to as XPF-ERCC1, to an XPF-depleted extract, ICL repair was not restored (Figure 2B). This could indicate that our XPF-ERCC1 complex was not active in ICL repair, or that XPF antibodies codepleted an unknown factor that is required for repair. To investigate the latter possibility, we raised an antibody against *xl*SLX4 (Figure S3A), a recently identified XPF interaction partner, and found that depletion of XPF-ERCC1 codepleted ~90% of SLX4. This indicates that the majority of SLX4 in our extracts resides in a stable complex with XPF-ERCC1 (Figure 2C). However, because there is more XPF-ERCC1 than SLX4 in extract, there is a large fraction of XPF-ERCC1 that is not in complex with SLX4 (Figures S1B and S3A). We also showed that FANCD2

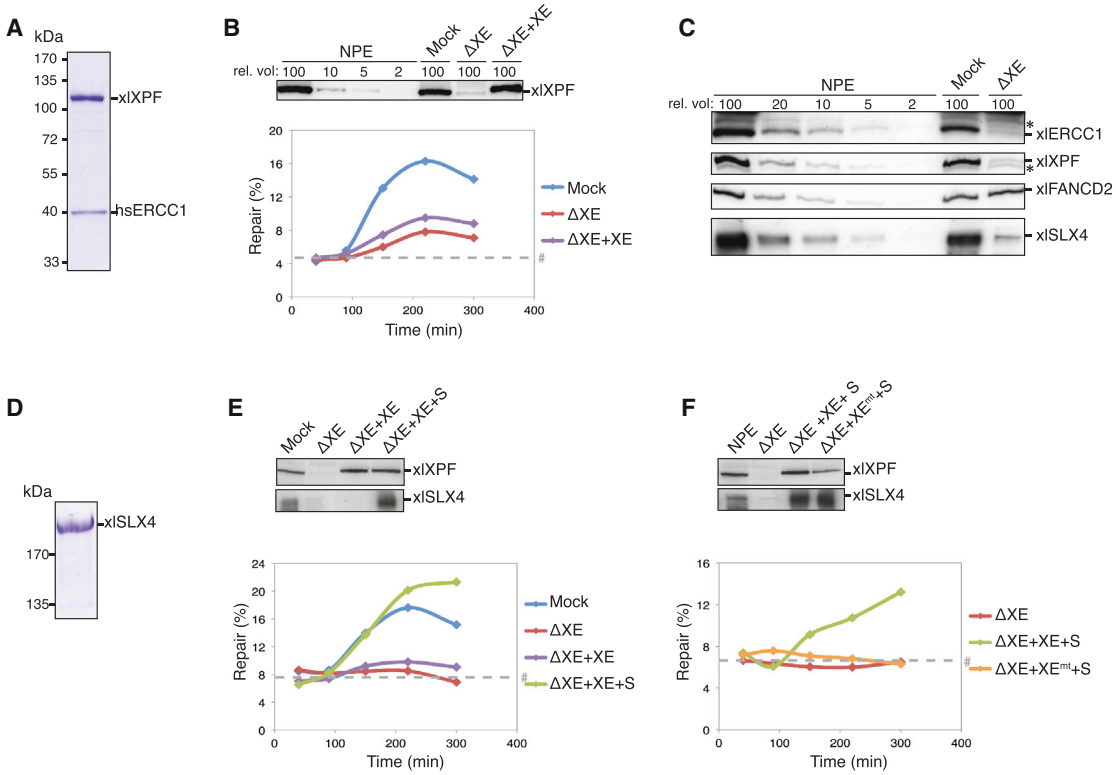

Figure 2. ICL Repair Defect after XPF-ERCC1 Depletion Is Rescued by Addition of XPF-ERCC1 in Combination with SLX4

(A) Recombinant *xl*XPF-*hs*ERCC1 complex was isolated via affinity purification using a FLAG tag on *xl*XPF and stained with Coomassie blue.

(B) Undepleted, mock-depleted, XPF-depleted (ΔXE), and XPF-depleted NPE complemented with the XPF-ERCC1 (ΔXE+XE) were analyzed by western blot using α-XPF antibody (upper panel). These extracts, with similarly treated HSS, were used to replicate pICL. Repair efficiency was calculated and plotted (lower panel).

(C) Undepleted, mock-depleted, and ERCC1-depleted NPE were analyzed by western blot using α-ERCC1, α-XPF, α-FANCD2, and α-SLX4 antibodies.

(D) *Xenopus laevis* SLX4 was purified via a FLAG tag and stained with Coomassie blue.

(E) Mock-depleted, ERCC1-depleted (ΔXE), and ERCC1-depleted NPE complemented with XPF-ERCC1 (ΔXE+XE) or XPF-ERCC1 and SLX4 (ΔXE+XE+S) were analyzed by western blot using α-XPF and α-SLX4 antibodies (upper panel). These extracts, with similarly treated HSS, were used to replicate pICL. Repair efficiency was calculated and plotted (lower panel).

(F) Undepleted, ERCC1-depleted (ΔXE), and ERCC1-depleted NPE complemented with XPF^{WT}-ERCC1 and SLX4 (ΔXE+XE+S) or XPF^{D668A}-ERCC1 and SLX4 ($\Delta XE+XE^{mt}+S$) were analyzed by western blot using α-XPF or α-SLX4 antibodies (upper panel). These extracts, with similarly treated HSS, were used to replicate pICL. Repair efficiency was calculated and plotted (lower panel). *, background band. #, SapI fragments from contaminating uncrosslinked plasmid present in varying degree in different pICL preparations. See also Figures S2 and S3.

is not part of this complex, as depletion of XPF-ERCC1 did not codeplete FANCD2 (Figure 2C). We then performed an ICL repair assay in ERCC1-depleted extract, to which we added recombinant XPF-ERCC1 or XPF-ERCC1 and recombinant SLX4 (Figure 2D). Strikingly, addition of XPF-ERCC1 and SLX4 rescued ICL repair (Figure 2E). When we used the nuclease-inactive form of XPF-ERCC1 in combination with SLX4, repair was not rescued (Figure 2F). Likewise, addition of SLX4 alone to an ERCC1-depleted extract did not rescue repair (Figure S3B). This shows that the nuclease activity of XPF-ERCC1 is required for ICL repair. We conclude that XPF-ERCC1 and SLX4 are both required for replication-coupled ICL repair.

Depletion of XPF-ERCC1 and SLX4 Specifically Inhibits the Incision Step in ICL Repair

We next examined whether XPF-ERCC1 is involved in ICL unhooking. To this end, we used an assay that monitors these incisions directly. We radioactively labeled pICL (pICL*) by nick-translation, which allowed us to specifically visualize the parental strands during ICL repair (Knipscheer et al., 2009). We replicated pICL* in mock-depleted and XPF-depleted extract and isolated repair intermediates at the indicated time points. These intermediates were linearized with HincII and separated on a denaturing agarose gel. In the mock-depleted extract, the linearized pICL* initially migrated as a large X-shaped molecule (Figures 3A, top, and 3B, lane 1). During ICL repair, incisions on both sides of the crosslink resulted in a decrease of the X-shaped structures and the formation of linear species and arms (Figures 3A, bottom, and 3B, lanes 2 and 3). The arms disappeared over time as the incised strands were repaired by HR, which resulted in further accumulation of linear fragments at later time points (Figures 1A and 3B, lanes 4 and 5). In addition, a fraction of the arms likely disappeared due to resection (Räschle et al., 2008). In the XPF-depleted extract, X-shaped products

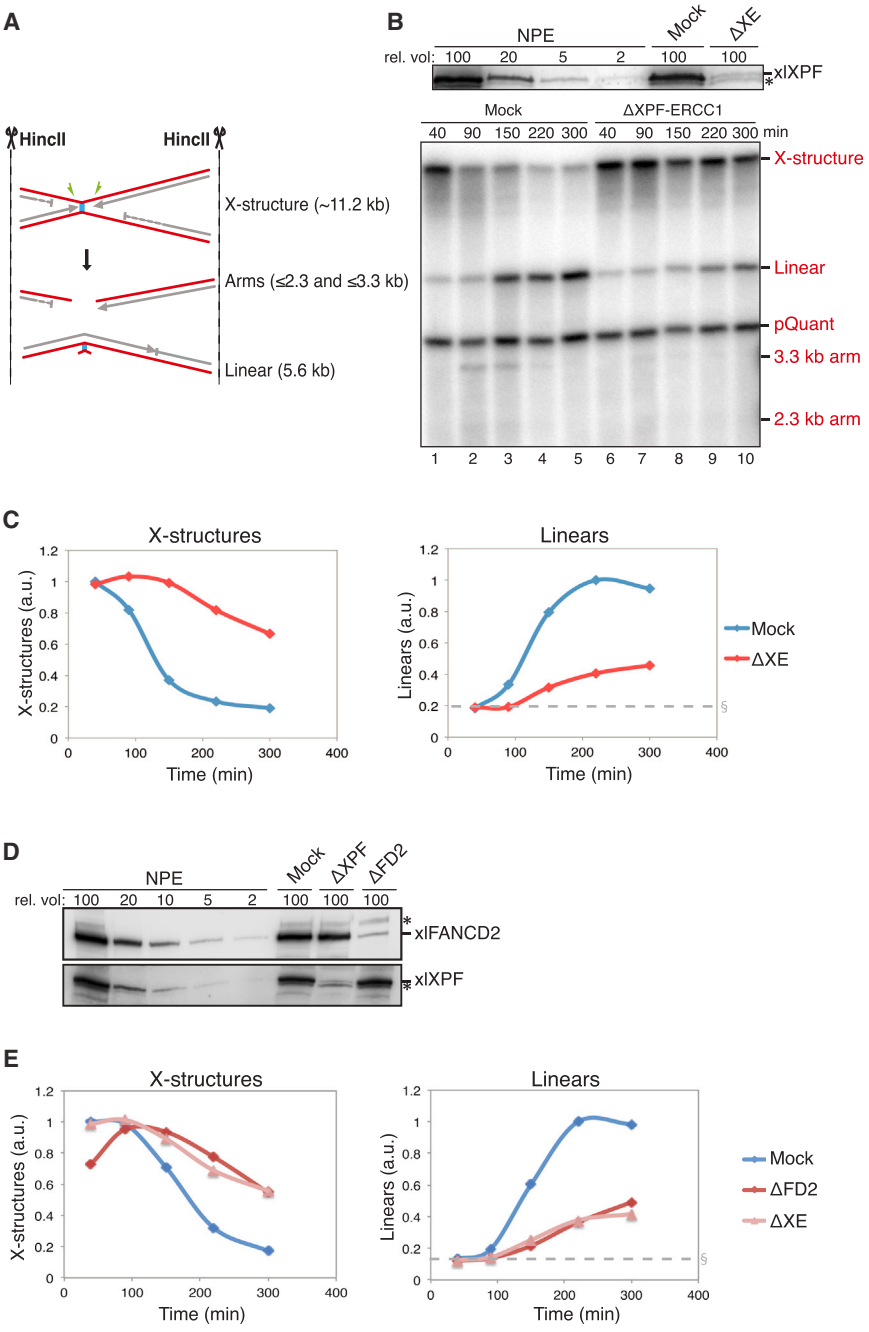

Figure 3. XPF-ERCC1 Depletion Inhibits Unhooking Incisions during ICL Repair

(A) Schematic representation of the incision assay. ^{32}P-α-deoxycytosine triphosphate-labeled parental strands are in red. Products before and after ICL incisions are indicated.

(B) Mock-depleted and XPF-depleted NPE were analyzed by western blot using α-XPF antibody (upper panel). Prelabeled pICL and pQuant were replicated in these extracts with similarly treated HSS. Replication products were isolated, digested by HincII, separated on a denaturing agarose gel, and visualized via autoradiography (lower panel).

(C) X-structures (left) and linear products (right) visualized in (B) were quantified and plotted.

(D) Mock-depleted, XPF-depleted (ΔXE), and FANCD2-depleted (ΔFD2) NPE were analyzed by western blot using α-XPF and α-FANCD2 antibodies (upper panel). Prelabeled pICL and pQuant were replicated in these extracts with similarly treated HSS. Replication products were analyzed as in (B), and X-structures and linear products were quantified and plotted (lower panels). *, background band. §, linear fragments from contaminating uncrosslinked plasmid present in pICL preparation. See also Figure S4.

persisted, and accumulation of linear products was strongly reduced (Figure 3B, lanes 6–10; see Figure 3C for quantification). This indicates that XPF-ERCC1 is required for the incision step in replication-coupled ICL repair. For comparison, FANCD2 depletion resulted in similar inhibition of incisions using this assay (Figures 3D and S4A) (Knipscheer et al., 2009).

To verify that the incision defect was caused by the depletion of XPF-ERCC1 and SLX4, we added XPF-ERCC1, or XPF-ERCC1 and SLX4, back to an ERCC1-depleted extract. As seen for the repair defect, only the readdition of XPF-ERCC1 in combination with SLX4 restored incisions (Figure 4A). Importantly, SLX4 alone or SLX4 in combination with XPF^{D668A}-ERCC1 did not rescue the incision defect (Figures 4B and S3C). This shows that the nuclease XPF-ERCC1 in combination with SLX4 specifically acts in the unhooking step in ICL repair.

Interestingly, we never observed an accumulation of Y-shaped products that would result from a single incision on pICL* (Figure S4B), indicating that XPF-ERCC1 makes both incisions or that the two incisions are functionally coupled, as in NER (see Discussion).

Based on experiments using immunoprecipitated proteins from cells, it has been suggested that SLX4 enhances the nuclease activity of XPF-ERCC1 (Muñoz et al., 2009). To test this using our proteins, we examined incision of stem-loop (Figure S2D), splayed arm (Figures S2E and S2F), and 3′ flap (Figures S2G and S2H) substrates and found no stimulation, but rather a slight inhibition of XPF-ERCC1-mediated incisions upon addition of SLX4.

FANCD2, XPF-ERCC1, and SLX4 Are Recruited to ICLs at the Time of Incisions

To further explore the mechanism of XPF-ERCC1- and SLX4-mediated incisions, we examined recruitment of XPF, SLX4, and FANCD2 to ICLs using chromatin immunoprecipitation (ChIP) (Fu et al., 2011; Long et al., 2011). We replicated pICL in *Xenopus* egg extracts, collected samples at various times, and

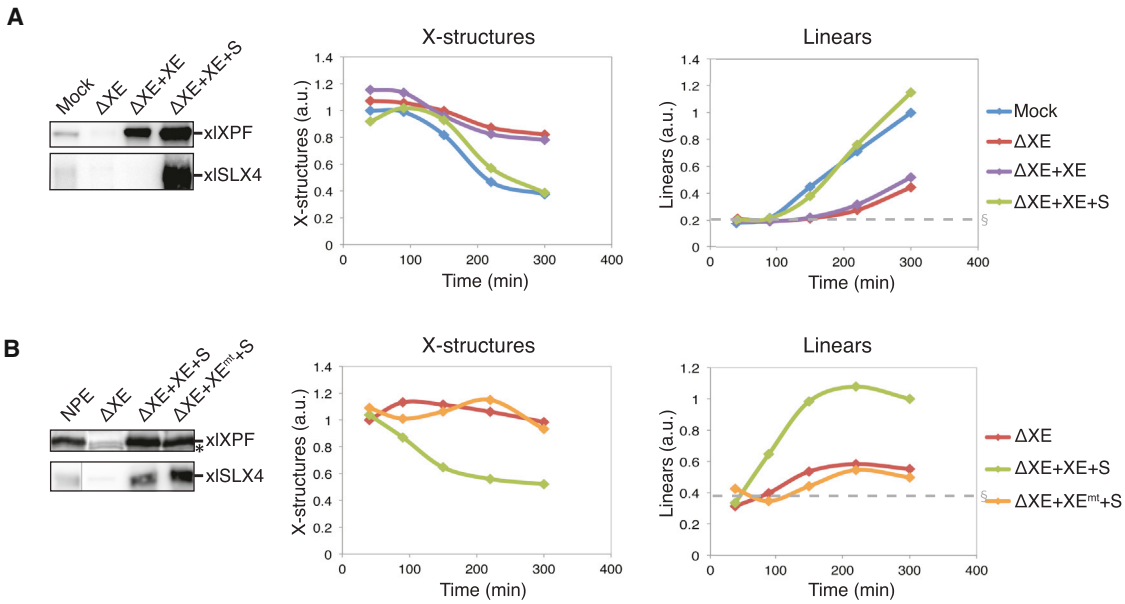

Figure 4. Unhooking Incisions during ICL Repair Require Both SLX4 and Nuclease Active XPF-ERCC1

(A) Mock-depleted, ERCC1-depleted (ΔXE), and ERCC1-depleted NPE complemented with XPF-ERCC1 (ΔXE+XE) or XPF-ERCC1 and SLX4 (ΔXE+XE+S) were analyzed by western blot using α-XPF and α-SLX4 antibodies (left panel). Prelabeled pICL and pQuant were replicated in these extracts with similarly treated HSS. Replication products were analyzed as in Figure 3B, and X-structures and linear products were quantified and plotted (right panels).

(B) Undepleted, ERCC1-depleted (ΔXE), or ERCC1-depleted NPE complemented with XPF^{WT}-ERCC1 and SLX4 (ΔXE+XE+S) or XPF^{D668A}-ERCC1 and SLX4 ($\Delta XE+XE^{mt}+S$) were analyzed by western blot using α-XPF and α-SLX4 antibodies (left panel). Prelabeled pICL and pQuant were replicated in these extracts with similarly treated HSS. Replication products were analyzed as in Figure 3B, and X-structures and linear products were quantified and plotted (right panels). §, linear fragments from contaminating uncrosslinked plasmid present in pICL preparation. See also Figure S3.

subjected these to protein-DNA crosslinking, sonication, and immunoprecipitation with FANCD2, XPF, and SLX4 antibodies. The DNA was recovered and amplified by quantitative PCR with primers specific to the ICL region (ICL), a region 700 nt from the ICL (MID), or a control region opposite the ICL (FAR) (Figure 5A). In addition, an unrelated plasmid (pQuant) was added to the reaction to assess protein recruitment to an undamaged, replicating molecule. To correlate the timing of FANCD2, XPF, and SLX4 recruitment to ICLs with the timing of key repair events, a parallel reaction was supplemented with ^{32}P-α-dCTP, and lesion bypass was analyzed on a sequencing gel. We showed previously that the majority of incisions occur after the leading strand reaches the −1 position, but before accumulation of the extension product (Figure 1A and Knipscheer et al., 2009). In this experiment, the majority of incisions took place between 50 and 120 min (Figure 5B). To verify our ChIP conditions, we first monitored the binding of MCM7, a subunit of the MCM2-7 helicase, to ICLs. As expected, accumulation of MCM7 at the ICL peaked ~12 min after NPE addition, when replication forks reached the ICL, and rapidly decreased thereafter (Figures 5B and 5C and Fu et al., 2011).

The direct binding of FANCD2 to ICLs has never been examined during replication-coupled ICL repair. We found that accumulation of FANCD2 at the ICL started at ~25 min and peaked at ~50 min (Figure 5D), coinciding with incisions and the kinetics of FANCD2 ubiquitylation (Knipscheer et al., 2009). Although FANCD2 was enriched at the ICL, we consistently also found FANCD2 at the MID and FAR loci (Figures 5D and S5A). In addition, we found that ~50 molecules of FANCD2 were ubiquitylated per ICL during repair (Figure S5B), indicating that one ICL was bound by many FANCD2 molecules. The recruitment of FANCD2 to the MID and FAR regions was slightly delayed compared to recruitment to the ICL. These results suggest that multiple molecules of FANCD2 bind to the ICL and subsequently spread to the surrounding DNA. To rule out that this effect was caused by incomplete sonication, we excluded all products longer than 400 bps from the PCR reaction, which did not reduce the binding of FANCD2 to MID and FAR regions (Figure S5C). This confirms that FANCD2 accumulates at the ICL during repair and spreads to the surrounding DNA. To investigate whether recruitment of FANCD2 depends on its ubiquitylation, we performed ChIP on repair reactions in FANCD2-depleted extract and FANCD2-depleted extract supplemented with WT or non-ubiquitylatable FANCD2 ($FANCD2^{K562R}$). As FANCD2 depletion leads to codepletion of FANCI (Knipscheer et al., 2009), we added FANCI-$FANCD2^{WT}$ or FANCI-$FANCD2^{K562R}$ complex. While the FANCI-$FANCD2^{WT}$ complex was efficiently recruited to the ICL, FANCI-$FANCD2^{K562R}$ did not bind above background levels observed in FANCD2-depleted extract (Figure S5D). We conclude that FANCD2 ubiquitylation is required for its recruitment to ICLs.

We next examined recruitment of XPF and SLX4 to pICL by ChIP. Both proteins were highly enriched at the ICL and, unlike FANCD2, did not bind above background to the MID and FAR regions (Figure S5C). We then analyzed the timing of recruitment of XPF and SLX4 to the ICL using samples from the

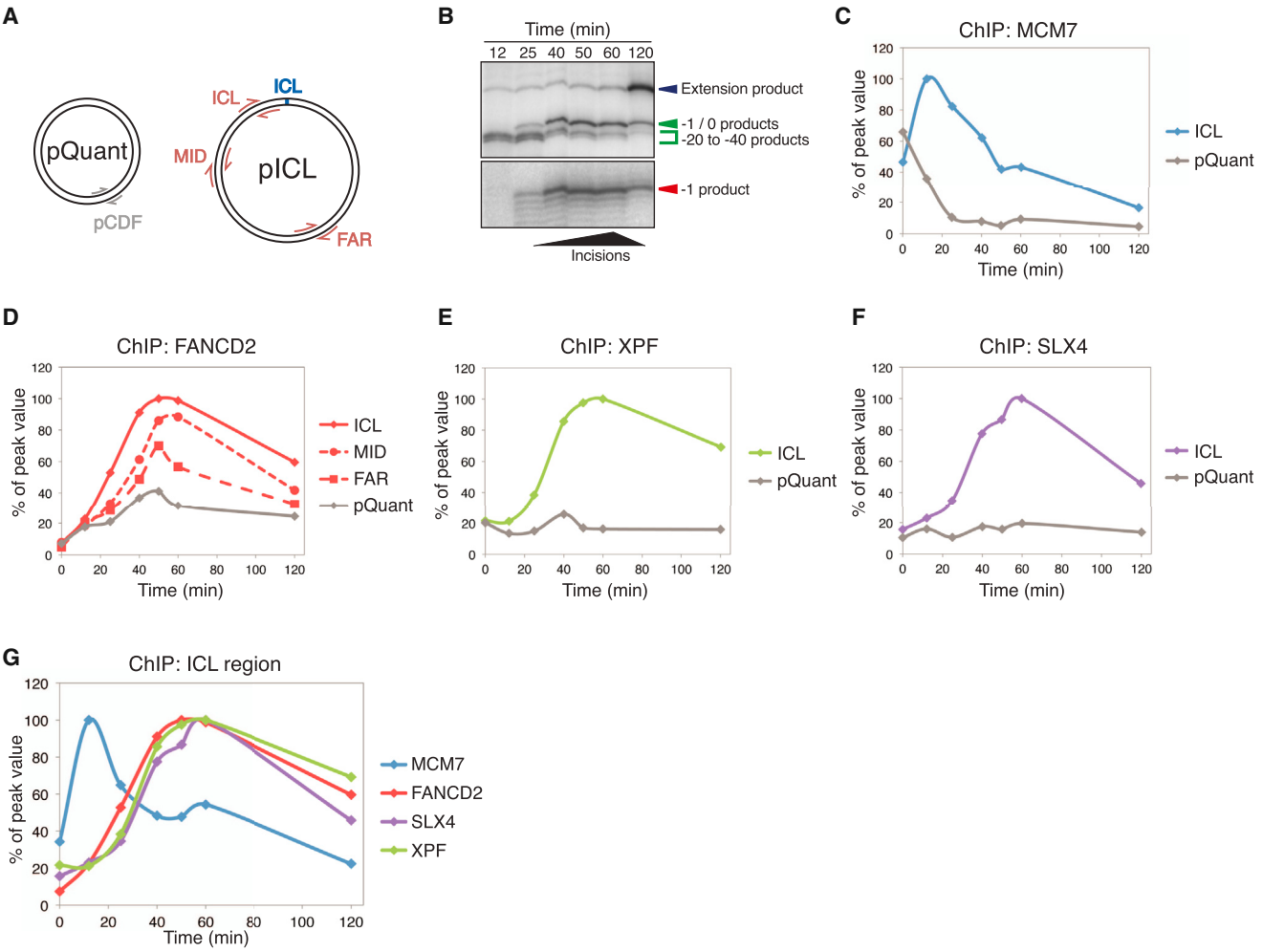

Figure 5. XPF and SLX4 Are Recruited to ICLs Shortly after FANCD2

(A) Schematic representation showing the primer locations on pICL—ICL (25–132 bp from ICL), MID (663–775 bp from ICL), FAR (2523–2622 bp from ICL)—and on pQuant.

(B) pICL was replicated in the presence of ^{32}P-α-deoxycytidine triphosphate. Repair intermediates were isolated, digested with AflIII, separated on a sequencing gel and visualized via autoradiography. The leading strand first stalls 20–40 nucleotides from the ICL (−20 to −40 products), after approach to the ICL it again stalls 1 nt from the ICL (−1 products). Full lesion bypass results in the "extension product." Timing of incisions is indicated below the gel ("incisions") (Knipscheer et al., 2009).

(C) Samples from parallel pICL replication reaction as in (B) were analyzed by MCM7 ChIP using ICL and pQuant primers. Initial MCM7 signal on pQuant is a result of MCM2-7 loading in HSS; during replication the signal decreases as the MCM2-7 helicase is displaced (Fu et al., 2011).

(D) Samples from parallel pICL replication reaction as in (B) were analyzed by FANCD2 ChIP using ICL, MID, FAR, and pQuant primers.

(E and F) Samples from parallel pICL replication reaction as in (B) were analyzed by XPF (E) and SLX4 (F) ChIP using ICL and pQuant primers.

(G) Combined graph for MCM7, FANCD2, XPF, and SLX4 ChIP using ICL primers. ChIP data are plotted as the percentage of peak value with the highest value set to 100%. See also Figures S5 and S6.

same replication reaction as described for FANCD2. XPF and SLX4 were recruited to the ICL with slightly delayed kinetics compared to FANCD2 (Figures 5E–5G and S5E). Thus, XPF and SLX4 are recruited to the ICL slightly after FANCD2 and coincident with incisions (Figures 5B and 5G). In summary, based on our finding that the large majority of SLX4 is in complex with XPF-ERCC1 (Figure 2C) and that SLX4 and XPF-ERCC1 load onto the ICL simultaneously, we conclude that the two proteins are most likely recruited as a complex after FANCD2.

FANCD2 Is Required for Efficient XPF-ERCC1 and SLX4 Recruitment to ICLs

To understand how XPF-ERCC1, SLX4, and FANCD2 are recruited to ICLs, we examined the interdependency of loading. We replicated pICL in mock-depleted, ERCC1-depleted, or ERCC1-depleted extract supplemented with XPF-ERCC1, SLX4, or both and analyzed the samples by ChIP (Figure S6A). While both XPF-ERCC1 and SLX4 were efficiently recruited to the ICL in the mock and dual add-back condition, loading of XPF-ERCC1 was strongly reduced in the absence of SLX4

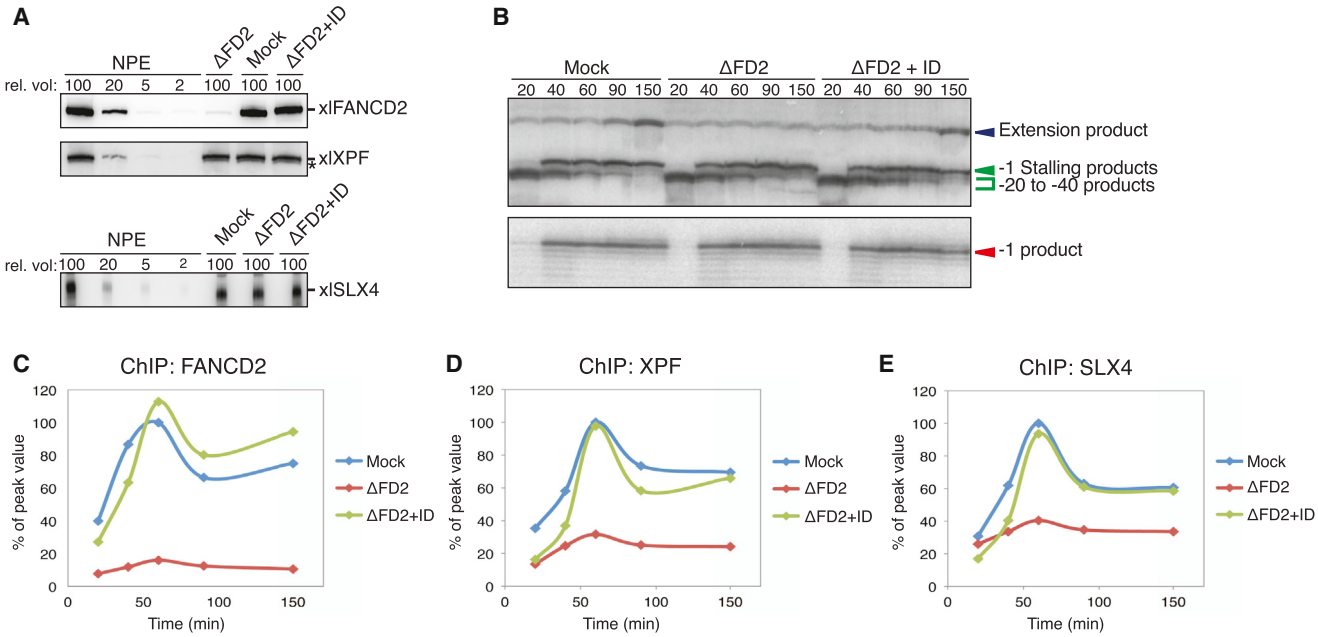

Figure 6. Efficient Recruitment of XPF and SLX4 to ICLs Depends on FANCD2

(A) Mock-depleted, FANCD2-depleted (ΔFD2), and FANCD2-depleted NPE complemented with FANCI-FANCD2 (ΔFD2+ID) were analyzed by western blot using α-FANCD2, α-XPF, and α-SLX4 antibodies.

(B) Extracts as described in (A) and similarly treated HSS were used to replicate plCL. Repair intermediates were isolated, digested with AflIII, separated on a sequencing gel, and visualized via autoradiography. Based on this lesion bypass assay, we infer that the majority of the incisions take place between 60 and 150 min in this experiment.

(C–E) Samples from parallel plCL replication reaction as in (B) were analyzed by FANCD2 (C), XPF (D), and SLX4 (E) ChIP using ICL primers. ChIP data are plotted as the percentage of peak value with the highest value set to 100%. *, background band. See also Figure S7.

(Figure S6B). In contrast, SLX4 was efficiently recruited to the ICL in the absence of XPF-ERCC1 (Figure S6C). This indicates that SLX4 functions to guide XPF-ERCC1 to its proper location. This is consistent with recent reports that show reduced ERCC1 foci and chromatin loading in the absence of SLX4 (Crossan et al., 2011; Kim et al., 2013; Stoepker et al., 2011). Interestingly, ERCC1 depletion did not affect the loading or spreading of FANCD2 (Figure S6D), indicating that FANCD2 loading occurs upstream of XPF-ERCC1 and SLX4 loading and incisions. Consistent with this, we found that ubiquitylation of FANCD2 is not affected by ERCC1 depletion (Figure S6E).

Because SLX4 and XPF-ERCC1 seem to act downstream of FANCD2, we questioned whether their recruitment depends on FANCD2. We replicated plCL in mock-depleted, FANCD2-depleted, and FANCD2-depleted extract supplemented with recombinant FANCI-FANCD2 (Figure 6A), and analyzed these samples by ChIP. In this experiment, lesion bypass (and therefore also incisions) occurred slightly later compared to the previous experiment using undepleted extract (Figures 5B and 6B). As expected, FANCD2 was not recruited to the ICL in FANCD2-depleted extract (Figure 6C). Notably, XPF recruitment was dramatically reduced after FANCD2 depletion, and this was fully reversed by FANCI-FANCD2 addition (Figures 6D, S7A, and S7B). FANCD2 depletion also caused a strong reduction of SLX4 recruitment that was rescued by addition of FANCI-FANCD2 complex (Figures 6E, S7A, and S7B). Importantly, neither XPF nor SLX4 were codepleted in FANCD2-depleted extracts (Figure 6A). In addition, nonubiquitylatable FANCD2 did not rescue recruitment of XPF and SLX4 to ICLs in FANCD2-depleted egg extract, consistent with our finding that this mutant does not bind to the ICL (Figures S7C and S5D). Taken together, these results show that the efficient recruitment of XPF-ERCC1 and SLX4 to ICLs depends on FANCD2 and its ubiquitylation, establishing a molecular link between FANCD2 and the unhooking step in replication-coupled ICL repair.

DISCUSSION

Over the past decade, at least four structure-specific endonucleases (XPF-ERCC1, MUS81-EME1, FAN1, SLX4-SLX1) have been heavily implicated in ICL repair. Among these, XPF was a strong candidate, given the fact it confers extreme cellular sensitivity to ICLs and its recent identification as a FANC protein (FANCQ) (Bogliolo et al., 2013; Kashiyama et al., 2013). Nevertheless, a direct demonstration that XPF is involved in ICL repair, as well as the step it catalyzes, were lacking. Here, we use a cell-free repair system with a chemically defined lesion to show that XPF-ERCC1 is responsible for the incisions that unhook the cross-linked nucleotide during replication-coupled ICL repair. We also show that FANCP/SLX4 is a critical regulator of XPF-ERCC1 in performing this reaction. Moreover, FANCD2 promotes the loading of SLX4 and XPF-ERCC1 at the ICL (Figure 7). These findings provide important insight into how the Fanconi anemia pathway directs a key step in replication-coupled ICL repair.

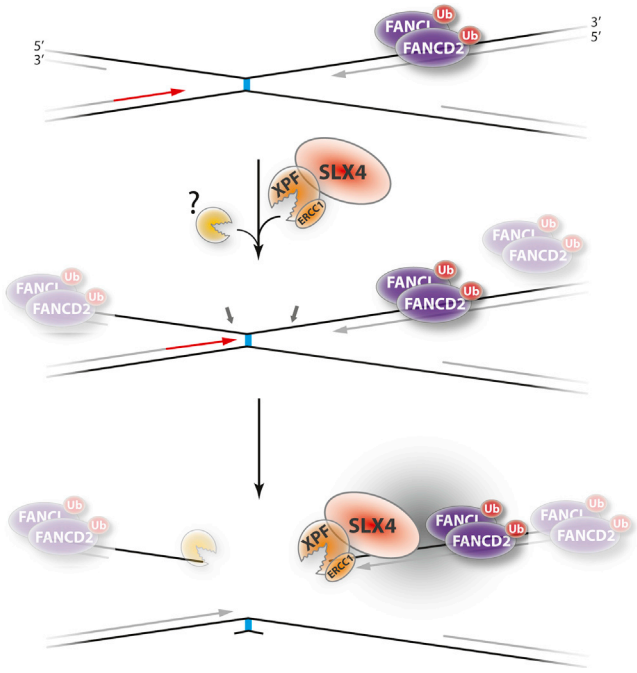

Figure 7. Model for XPF-ERCC1-Dependent Incision(s) Mediated by SLX4 and Ubiquitylated FANCI-FANCD2

XPF-ERCC1 is recruited to the ICL by SLX4 and most likely makes the 3′ flap incision. The 5′ flap incision could also be made by XPF-ERCC1 or by a currently unknown endonuclease (yellow). FANCD2 and its ubiquitylation are required for the efficient recruitment of XPF-ERCC1 and SLX4 to the ICL. This could be through a direct interaction, through interaction mediated by an additional protein, or by creating an appropriate DNA structure. After loading at the ICL, FANCD2 spreads throughout the surrounding DNA (faded FANCI-FANCD2 complexes).

It has long been debated which endonucleases perform the unhooking incisions in ICL repair. Our data not only demonstrate that XPF-ERCC1 is directly required for unhooking (Figure 7), but also suggest that neither MUS81-EME1 nor FAN1 is essential for this process (Figure 1). The reported function of MUS81 in processing persistent stalled replication forks could account for the decrease in DSBs observed after ICL treatment in the absence of MUS81 (Naim et al., 2013; Szakal and Branzei, 2013). In support of this view, it was recently reported that MUS81 promotes DSBs when ICLs persist (Wang et al., 2011). A major role for the 5′ endonuclease FAN1 (Kratz et al., 2010; Liu et al., 2010; MacKay et al., 2010; Smogorzewska et al., 2010) in the FA pathway has recently been questioned (Trujillo et al., 2012). Although we found that FAN1 depletion had no effect on ICL repair, FAN1 could function redundantly with another 5′ endonuclease, possibly SLX1. With XPF performing the 3′ incision (Figure 7), this model would be in agreement with current views that the two incisions are performed by different structure-specific endonucleases. Interestingly, the fact that depletion of XPF-ERCC1 abolishes both of the unhooking incisions, and that a catalytic mutant of XPF does not support any incision (Figure 4), suggests that the 5′ incision depends critically on the 3′ incision. This view is analogous to NER, where the 5′ incision by XPG is dependent on XPF-ERCC1 performing the 3′ incision (Staresincic et al., 2009). An alternative model suggests that the exonuclease activity of SNM1A supports resection of DNA past the ICL starting from a nick made by XPF-ERCC1 (Wang et al., 2011). Interestingly, this model would be consistent with XPF-ERCC1 making the first incision. Another mechanism that is consistent with our data is that XPF-ERCC1 makes both the unhooking incisions. This model has been suggested previously based on experiments with fork-like DNA templates and purified XPF-ERCC1 protein (Fisher et al., 2008; Kuraoka et al., 2000), and further evidence for such a model is presented in Hodskinson et al. (2014).

Although mutations in *SLX4/FANCP* cause FA and cellular sensitivity for ICL-inducing agents, a role for this protein in ICL repair has not been defined. The interaction domain of SLX4 with XPF-ERCC1 is important to confer resistance to ICL-inducing agents, and SLX4 colocalizes with XPF-ERCC1 in nuclear foci (Crossan et al., 2011; Fekairi et al., 2009; Kim et al., 2013; Muñoz et al., 2009; Stoepker et al., 2011; Svendsen et al., 2009), suggesting that the interaction with XPF is important for the function of SLX4 in ICL repair. In addition, Fanconi patients with a defect in SLX4 show a phenotype more comparable to patients with a defect in components of the FA core complex, or FANCI/FANCD2, than to patients with defects in HR-related FA proteins (Kim et al., 2011). Our data showing that SLX4 is crucial for the XPF-ERCC1-dependent unhooking incisions (Figure 4) explain these previous observations and establish a specific function for SLX4 in ICL repair. We demonstrate that SLX4 is specifically recruited to the ICL during repair, and although SLX4 can bind the ICL independently of XPF-ERCC1 (Figure S6), normally SLX4 and XPF-ERCC1 are most likely recruited as a complex (Figure 7). This is based on our observation that the majority of SLX4 binds XPF-ERCC1 in *Xenopus* egg extract and that both proteins are recruited to ICLs with very similar kinetics (Figures 2 and 5). In addition to a role for SLX4 in recruiting XPF-ERCC1 to the site of damage, SLX4 could also stimulate XPF-ERCC1 nuclease activity. Although we do not observe stimulation of XPF-ERCC1 by SLX4 on a variety of DNA substrates (Figure S2), this has been observed with a truncated form of SLX4 (Hodskinson et al., 2014). Hodskinson et al. copurified truncated SLX4 with XPF-ERCC1, while our full-length SLX4 was purified separately. Although our SLX4 is fully functional in *Xenopus* egg extract, copurification with XPF-ERCC1 could be necessary to induce an active conformation that stimulates cleavage of a model substrate in isolation.

Another interesting question is how SLX4 and XPF-ERCC1 are recruited to ICLs. While some reports suggest a direct interaction between ubiquitylated FANCD2 and the UBZ domains of SLX4 (Yamamoto et al., 2011), others show that the UBZ domains of SLX4 are not required for its recruitment to foci (Kim et al., 2013). We show that efficient binding of SLX4 and XPF-ERCC1 to ICLs during repair depends on FANCD2 and its ubiquitylation (Figures 6 and S5), but whether this is mediated by a direct interaction is unclear (Figure 7). Interestingly, we find that FANCD2 is not only recruited to the ICL but also to the DNA surrounding the ICL (Figures 5 and S5). As this spreading behavior was also seen for Rad51 (Long et al., 2011), we hypothesize that FANCD2 has an additional role in HR. Alternatively, spreading could serve as a signal to mark the region around

the damage site, similar to phosphorylation of H2AX in DSB repair. Because XPF-ERCC1 and SLX4 do not spread, but bind specifically to the ICL (Figure S5), we hypothesize that an additional factor cooperates with FANCI-FANCD2 to recruit the nuclease complex to the lesion. Given the importance of the UBZ domain of SLX4 in conferring resistance to ICL-inducing agents (Kim et al., 2011), we speculate this unknown protein could be ubiquitylated. In summary, by showing that XPF-ERCC1, together with SLX4, is responsible for the incision step in ICL repair, and exploring how these proteins are recruited to the site of damage by the FA pathway, we have shed important light on a key event in this replication-coupled repair pathway.

EXPERIMENTAL PROCEDURES

Xenopus Egg Extracts and DNA Replication and Repair Assay

Animal experiments were performed in accordance with the rules of the Animal Experimentation Committee of the Royal Netherlands Academy of Arts and Sciences (DEC-KNAW). DNA replication and preparation of *Xenopus* egg extracts were performed as described (Tutter and Walter, 2006; Walter et al., 1998). Preparation of plasmid with a site-specific cisplatin ICL (pICL) and ICL repair assays were performed as described (Enoiu et al., 2012; Räschle et al., 2008). Briefly, pICL was incubated with HSS for 20 min, following addition of two volumes of NPE (t = 0) containing ^{32}P-α-dCTP. Aliquots of replication reaction (4–10 μl) were stopped at various times with ten volumes of Stop Solution II (0.5% SDS, 10 mM EDTA, 50 mM Tris [pH 7.5]). Samples were incubated with RNase (0.13 μg/μl) followed by Proteinase K (0.5 μg/μl) for 30 min at 37°C each. DNA was phenol/chloroform extracted, ethanol precipitated in the presence of glycogen (30 mg/ml), and resuspended in 5–10 μl of 10 mM Tris (pH 7.5). ICL repair was analyzed by digesting 1 μl of DNA with HincII or HincII and SapI, separation on a 0.8% native agarose gel, and quantification using autoradiography. Repair efficiency was calculated as described (Knipscheer et al., 2009).

Antibodies and Immunodepletions

FANCD2 and MCM7 antibodies were described previously (Räschle et al., 2008; Walter and Newport, 2000). Antibodies were raised against residues 444–797 of *xl*XPF, full-length *xl*ERCC1, residues 1–208 of *xl*FAN1, residues 1–231 of *xl*MUS81, and residues 825–1052 of *xl*SLX4. XPF-ERCC1 was removed from extract using two rounds of depletion with the α-XPF serum (HSS and NPE) or with two or three rounds of depletion with the α-ERCC1 serum (HSS and NPE, respectively). FAN1 and MUS81 were removed from extract using two rounds of depletion (HSS and NPE). FANCD2 depletion was as described (Knipscheer et al., 2009).

Protein Purification

*xl*FANCI-*xl*FANCD2 was prepared as previously described (Knipscheer et al., 2009). *xl*XPF-*hs*ERCC1, *hs*XPF-*hs*ERCC1, and *xl*SLX4 were prepared using similar procedures. Briefly, FLAG-tagged XPF and His-tagged ERCC1 were coexpressed, and FLAG-tagged SLX4 was expressed in Sf9 cells and affinity purified using FLAG-M2 affinity gel. GST-tagged FAN1 was expressed in Sf9 cells and affinity purified using Gluthathion Sepharose 4B. The GST tag was removed using PreScission Protease.

Incision Assay

pICL and pQuant were labeled via nick-translation (Knipscheer et al., 2009). pQuant was added to correct for variation in extraction. pICL (225 ng) and pQuant (11.25 ng) were incubated in 1.5 units of NB-BSR DI enzyme (NEB) and NEBuffer2 for 30 min at room temperature. Subsequently, 11 μl DNA Polymerase mix (5 units DNA Polymerase I [NEB], dATP, dGTP, dTTP [0.5 mM each], dCTP [0.4 μM], ^{32}P-α-dCTP [3.3 μM] in NEBuffer2) was added and incubated for 3 min at 16°C. The reaction was stopped with 180 μl Stop Solution II, Proteinase K treated, and phenol/chloroform extracted. Excess label was removed using a Bio-Spin 6 Column (Bio-Rad). After ethanol precipitation, the pellet was resuspended in 5 μl ELB (10 mM HEPES-KOH [pH 7.7], 50 mM KCl, 2.5 mM $MgCl_2$, 250 mM sucrose). The labeled plasmid (pICL*) was used for replication, and samples at various times were extracted and digested with HincII. Fragments were separated on a 0.8% alkaline denaturing agarose gel for 18 hr at 0.85 volts/cm, after which the gel was dried and exposed to a phosphor-screen. Quantification was performed using ImageQuant software (GE Healthcare).

Nascent Strand Analysis

Nascent strand analysis was performed as described (Räschle et al., 2008). Briefly, DNA replication products were extracted and digested with AflIII. Gel Loading Buffer II (Life Technologies) was added, and the fragments were separated on a 7% polyacrylamide sequencing gel. The gel was transferred to filter paper, dried, and visualized using autoradiography.

Chromatin Immunoprecipitation

ChIP was performed as described (Pacek et al., 2006). Briefly, reaction samples were crosslinked with formaldehyde, sonicated to yield DNA fragments of 100–500 bp, and immunoprecipitated with the indicated antibodies. Protein-DNA crosslinks were reversed, and DNA was phenol/chloroform extracted for analysis by quantitative real-time PCR with the following primers: ICL (5′-AGCCAGATTTTTCCTCCTCTC-3′ and 5′-CATGCATTGGTTCTGC ACTT-3′), MID (5′-ACCCTGGGTTCTTTTCCAAC-3′ and 5′-CATTTCATCTGGA GCGTCCT-3′), FAR (5′-AACGCCAATAGGGACTTTCC-3′ and 5′-GGGCGTA CTTGGCATATGAT-3′), and pQant (5′-TACAAATGTACGGCCAGCAA-3′ and 5′-GAGTATGAGGGAAGCGGTGA-3′).

Accesion Numbers

The NCBI Genbank accession numbers for the *Xenopus FAN1*, *SLX4*, and *MUS81* cDNA sequences reported in this paper are KJ473955, KJ473956, KJ473957, respectively.

SUPPLEMENTAL INFORMATION

Supplemental Information includes seven figures and Supplemental Experimental Procedures and can be found with this article online at http://dx.doi.org/10.1016/j.molcel.2014.03.015.

AUTHOR CONTRIBUTIONS

D.K.D. and R.A.C.M.B performed most of the experiments, each with equal contributions.

ACKNOWLEDGMENTS

This work was supported by the Netherlands organization for Scientific Research (VIDI 700.10.421 to P.K.), a Dutch Cancer Society Fellowship (to P.K.), a National Institutes of Health Grant (HL098316) to J.C.W., and an American Cancer Society postdoctoral fellowship (PF-10-146-01-DMC) and NIH award (K99GM102325) to D.T.L.. M.R. was supported by the Center for Integrated Protein Science Munich (CIPSM). We thank R. Kanaar for human *XPF* cDNA, W. Hoogenboom and P. Castillo Bosch for analyzing ChIP samples, the Hubrecht animal caretakers for animal support, and the Knipscheer and Walter laboratories for feedback.

Received: October 7, 2013
Revised: January 17, 2014
Accepted: February 28, 2014
Published: April 10, 2014

REFERENCES

Adair, G.M., Rolig, R.L., Moore-Faver, D., Zabelshansky, M., Wilson, J.H., and Nairn, R.S. (2000). Role of ERCC1 in removal of long non-homologous tails during targeted homologous recombination. EMBO J. *19*, 5552–5561.

Bergstralh, D.T., and Sekelsky, J. (2008). Interstrand crosslink repair: can XPF-ERCC1 be let off the hook? Trends Genet. *24*, 70–76.

Bogliolo, M., Schuster, B., Stoepker, C., Derkunt, B., Su, Y., Raams, A., Trujillo, J.P., Minguillón, J., Ramírez, M.J., Pujol, R., et al. (2013). Mutations in ERCC4, encoding the DNA-repair endonuclease XPF, cause Fanconi anemia. Am. J. Hum. Genet. *92*, 800–806.

Castor, D., Nair, N., Déclais, A.C., Lachaud, C., Toth, R., Macartney, T.J., Lilley, D.M., Arthur, J.S., and Rouse, J. (2013). Cooperative control of holliday junction resolution and DNA repair by the SLX1 and MUS81-EME1 nucleases. Mol. Cell *52*, 221–233.

Chen, X.B., Melchionna, R., Denis, C.M., Gaillard, P.H., Blasina, A., Van de Weyer, I., Boddy, M.N., Russell, P., Vialard, J., and McGowan, C.H. (2001). Human Mus81-associated endonuclease cleaves Holliday junctions in vitro. Mol. Cell *8*, 1117–1127.

Ciccia, A., McDonald, N., and West, S.C. (2008). Structural and functional relationships of the XPF/MUS81 family of proteins. Annu. Rev. Biochem. *77*, 259–287.

Crossan, G.P., van der Weyden, L., Rosado, I.V., Langevin, F., Gaillard, P.H., McIntyre, R.E., Gallagher, F., Kettunen, M.I., Lewis, D.Y., Brindle, K., et al.; Sanger Mouse Genetics Project (2011). Disruption of mouse Slx4, a regulator of structure-specific nucleases, phenocopies Fanconi anemia. Nat. Genet. *43*, 147–152.

De Silva, I.U., McHugh, P.J., Clingen, P.H., and Hartley, J.A. (2000). Defining the roles of nucleotide excision repair and recombination in the repair of DNA interstrand cross-links in mammalian cells. Mol. Cell. Biol. *20*, 7980–7990.

Dronkert, M.L., de Wit, J., Boeve, M., Vasconcelos, M.L., van Steeg, H., Tan, T.L., Hoeijmakers, J.H., and Kanaar, R. (2000). Disruption of mouse SNM1 causes increased sensitivity to the DNA interstrand cross-linking agent mitomycin C. Mol. Cell. Biol. *20*, 4553–4561.

Enoiu, M., Jiricny, J., and Schärer, O.D. (2012). Repair of cisplatin-induced DNA interstrand crosslinks by a replication-independent pathway involving transcription-coupled repair and translesion synthesis. Nucleic Acids Res. *40*, 8953–8964.

Enzlin, J.H., and Schärer, O.D. (2002). The active site of the DNA repair endonuclease XPF-ERCC1 forms a highly conserved nuclease motif. EMBO J. *21*, 2045–2053.

Fekairi, S., Scaglione, S., Chahwan, C., Taylor, E.R., Tissier, A., Coulon, S., Dong, M.Q., Ruse, C., Yates, J.R., 3rd, Russell, P., et al. (2009). Human SLX4 is a Holliday junction resolvase subunit that binds multiple DNA repair/recombination endonucleases. Cell *138*, 78–89.

Fisher, L.A., Bessho, M., and Bessho, T. (2008). Processing of a psoralen DNA interstrand cross-link by XPF-ERCC1 complex in vitro. J. Biol. Chem. *283*, 1275–1281.

Fu, Y.V., Yardimci, H., Long, D.T., Ho, T.V., Guainazzi, A., Bermudez, V.P., Hurwitz, J., van Oijen, A., Schärer, O.D., and Walter, J.C. (2011). Selective bypass of a lagging strand roadblock by the eukaryotic replicative DNA helicase. Cell *146*, 931–941.

Hanada, K., Budzowska, M., Modesti, M., Maas, A., Wyman, C., Essers, J., and Kanaar, R. (2006). The structure-specific endonuclease Mus81-Eme1 promotes conversion of interstrand DNA crosslinks into double-strands breaks. EMBO J. *25*, 4921–4932.

Hodskinson, M.R.G., Silhan, J., Crossan, G.P., Garaycoechea, J.I., Mukherjee, S., Johnson, C.M., Schärer, O.D., and Patel, K.J. (2014). Mouse SLX4 Is a Tumor Suppressor that Stimulates the Activity of the Nuclease XPF-ERCC1 in DNA Crosslink Repair. Mol. Cell *54*, this issue, 472–484.

Howlett, N.G., Taniguchi, T., Olson, S., Cox, B., Waisfisz, Q., De Die-Smulders, C., Persky, N., Grompe, M., Joenje, H., Pals, G., et al. (2002). Biallelic inactivation of BRCA2 in Fanconi anemia. Science *297*, 606–609.

Kashiyama, K., Nakazawa, Y., Pilz, D.T., Guo, C., Shimada, M., Sasaki, K., Fawcett, H., Wing, J.F., Lewin, S.O., Carr, L., et al. (2013). Malfunction of nuclease ERCC1-XPF results in diverse clinical manifestations and causes Cockayne syndrome, xeroderma pigmentosum, and Fanconi anemia. Am. J. Hum. Genet. *92*, 807–819.

Kim, Y., Lach, F.P., Desetty, R., Hanenberg, H., Auerbach, A.D., and Smogorzewska, A. (2011). Mutations of the SLX4 gene in Fanconi anemia. Nat. Genet. *43*, 142–146.

Kim, H., Yang, K., Dejsuphong, D., and D'Andrea, A.D. (2012). Regulation of Rev1 by the Fanconi anemia core complex. Nat. Struct. Mol. Biol. *19*, 164–170.

Kim, Y., Spitz, G.S., Veturi, U., Lach, F.P., Auerbach, A.D., and Smogorzewska, A. (2013). Regulation of multiple DNA repair pathways by the Fanconi anemia protein SLX4. Blood *121*, 54–63.

Knipscheer, P., Räschle, M., Smogorzewska, A., Enoiu, M., Ho, T.V., Schärer, O.D., Elledge, S.J., and Walter, J.C. (2009). The Fanconi anemia pathway promotes replication-dependent DNA interstrand cross-link repair. Science *326*, 1698–1701.

Knipscheer, P., Räschle, M., Schärer, O.D., and Walter, J.C. (2012). Replication-coupled DNA interstrand cross-link repair in Xenopus egg extracts. Methods Mol. Biol. *920*, 221–243.

Kottemann, M.C., and Smogorzewska, A. (2013). Fanconi anaemia and the repair of Watson and Crick DNA crosslinks. Nature *493*, 356–363.

Kratz, K., Schöpf, B., Kaden, S., Sendoel, A., Eberhard, R., Lademann, C., Cannavó, E., Sartori, A.A., Hengartner, M.O., and Jiricny, J. (2010). Deficiency of FANCD2-associated nuclease KIAA1018/FAN1 sensitizes cells to interstrand crosslinking agents. Cell *142*, 77–88.

Kuraoka, I., Kobertz, W.R., Ariza, R.R., Biggerstaff, M., Essigmann, J.M., and Wood, R.D. (2000). Repair of an interstrand DNA cross-link initiated by ERCC1-XPF repair/recombination nuclease. J. Biol. Chem. *275*, 26632–26636.

Liu, T., Ghosal, G., Yuan, J., Chen, J., and Huang, J. (2010). FAN1 acts with FANCI-FANCD2 to promote DNA interstrand cross-link repair. Science *329*, 693–696.

Long, D.T., Räschle, M., Joukov, V., and Walter, J.C. (2011). Mechanism of RAD51-dependent DNA interstrand cross-link repair. Science *333*, 84–87.

MacKay, C., Déclais, A.C., Lundin, C., Agostinho, A., Deans, A.J., MacArtney, T.J., Hofmann, K., Gartner, A., West, S.C., Helleday, T., et al. (2010). Identification of KIAA1018/FAN1, a DNA repair nuclease recruited to DNA damage by monoubiquitinated FANCD2. Cell *142*, 65–76.

Muñoz, I.M., Hain, K., Déclais, A.C., Gardiner, M., Toh, G.W., Sanchez-Pulido, L., Heuckmann, J.M., Toth, R., Macartney, T., Eppink, B., et al. (2009). Coordination of structure-specific nucleases by human SLX4/BTBD12 is required for DNA repair. Mol. Cell *35*, 116–127.

Naim, V., Wilhelm, T., Debatisse, M., and Rosselli, F. (2013). ERCC1 and MUS81-EME1 promote sister chromatid separation by processing late replication intermediates at common fragile sites during mitosis. Nat. Cell Biol. *15*, 1008–1015.

Niedernhofer, L.J., Odijk, H., Budzowska, M., van Drunen, E., Maas, A., Theil, A.F., de Wit, J., Jaspers, N.G., Beverloo, H.B., Hoeijmakers, J.H., and Kanaar, R. (2004). The structure-specific endonuclease Ercc1-Xpf is required to resolve DNA interstrand cross-link-induced double-strand breaks. Mol. Cell. Biol. *24*, 5776–5787.

Osman, F., and Whitby, M.C. (2007). Exploring the roles of Mus81-Eme1/Mms4 at perturbed replication forks. DNA Repair (Amst.) *6*, 1004–1017.

Pacek, M., Tutter, A.V., Kubota, Y., Takisawa, H., and Walter, J.C. (2006). Localization of MCM2-7, Cdc45, and GINS to the site of DNA unwinding during eukaryotic DNA replication. Mol. Cell *21*, 581–587.

Räschle, M., Knipscheer, P., Enoiu, M., Angelov, T., Sun, J., Griffith, J.D., Ellenberger, T.E., Schärer, O.D., and Walter, J.C. (2008). Mechanism of replication-coupled DNA interstrand crosslink repair. Cell *134*, 969–980.

Schiestl, R.H., and Prakash, S. (1990). RAD10, an excision repair gene of Saccharomyces cerevisiae, is involved in the RAD1 pathway of mitotic recombination. Mol. Cell. Biol. *10*, 2485–2491.

Smogorzewska, A., Desetty, R., Saito, T.T., Schlabach, M., Lach, F.P., Sowa, M.E., Clark, A.B., Kunkel, T.A., Harper, J.W., Colaiácovo, M.P., and Elledge, S.J. (2010). A genetic screen identifies FAN1, a Fanconi anemia-associated nuclease necessary for DNA interstrand crosslink repair. Mol. Cell *39*, 36–47.

Staresincic, L., Fagbemi, A.F., Enzlin, J.H., Gourdin, A.M., Wijgers, N., Dunand-Sauthier, I., Giglia-Mari, G., Clarkson, S.G., Vermeulen, W., and

Schärer, O.D. (2009). Coordination of dual incision and repair synthesis in human nucleotide excision repair. EMBO J. *28*, 1111–1120.

Stoepker, C., Hain, K., Schuster, B., Hilhorst-Hofstee, Y., Rooimans, M.A., Steltenpool, J., Oostra, A.B., Eirich, K., Korthof, E.T., Nieuwint, A.W., et al. (2011). SLX4, a coordinator of structure-specific endonucleases, is mutated in a new Fanconi anemia subtype. Nat. Genet. *43*, 138–141.

Svendsen, J.M., Smogorzewska, A., Sowa, M.E., O'Connell, B.C., Gygi, S.P., Elledge, S.J., and Harper, J.W. (2009). Mammalian BTBD12/SLX4 assembles a Holliday junction resolvase and is required for DNA repair. Cell *138*, 63–77.

Szakal, B., and Branzei, D. (2013). Premature Cdk1/Cdc5/Mus81 pathway activation induces aberrant replication and deleterious crossover. EMBO J. *32*, 1155–1167.

Thompson, L.H., and Hinz, J.M. (2009). Cellular and molecular consequences of defective Fanconi anemia proteins in replication-coupled DNA repair: mechanistic insights. Mutat. Res. *668*, 54–72.

Trujillo, J.P., Mina, L.B., Pujol, R., Bogliolo, M., Andrieux, J., Holder, M., Schuster, B., Schindler, D., and Surrallés, J. (2012). On the role of FAN1 in Fanconi anemia. Blood *120*, 86–89.

Tutter, A.V., and Walter, J.C. (2006). Chromosomal DNA replication in a soluble cell-free system derived from Xenopus eggs. Methods Mol. Biol. *322*, 121–137.

Walter, J., and Newport, J. (2000). Initiation of eukaryotic DNA replication: origin unwinding and sequential chromatin association of Cdc45, RPA, and DNA polymerase alpha. Mol. Cell *5*, 617–627.

Walter, J., Sun, L., and Newport, J. (1998). Regulated chromosomal DNA replication in the absence of a nucleus. Mol. Cell *1*, 519–529.

Wang, A.T., Sengerová, B., Cattell, E., Inagawa, T., Hartley, J.M., Kiakos, K., Burgess-Brown, N.A., Swift, L.P., Enzlin, J.H., Schofield, C.J., et al. (2011). Human SNM1A and XPF-ERCC1 collaborate to initiate DNA interstrand cross-link repair. Genes Dev. *25*, 1859–1870.

Williams, H.L., Gottesman, M.E., and Gautier, J. (2012). Replication-independent repair of DNA interstrand crosslinks. Mol. Cell *47*, 140–147.

Wood, R.D. (2010). Mammalian nucleotide excision repair proteins and interstrand crosslink repair. Environ. Mol. Mutagen. *51*, 520–526.

Yamamoto, K.N., Kobayashi, S., Tsuda, M., Kurumizaka, H., Takata, M., Kono, K., Jiricny, J., Takeda, S., and Hirota, K. (2011). Involvement of SLX4 in interstrand cross-link repair is regulated by the Fanconi anemia pathway. Proc. Natl. Acad. Sci. USA *108*, 6492–6496.

Zheng, L., Dai, H., Zhou, M., Li, M., Singh, P., Qiu, J., Tsark, W., Huang, Q., Kernstine, K., Zhang, X., et al. (2007). Fen1 mutations result in autoimmunity, chronic inflammation and cancers. Nat. Med. *13*, 812–819.